

April 10, 2017

# Kinetics of the Crystalline Nuclei Growth in Glassy Systems

Anatolii V. Mokshin\* and Bulat N. Galimzyanov

*Department of Computational Physics, Institute of Physics,**Kazan Federal University, 420008 Kazan, Russia and**Landau Institute for Theoretical Physics, Russian Academy of Sciences, 142432 Chernogolovka, Russia*

In this work, we study the crystalline nuclei growth in glassy systems focusing primarily on the early stages of the process, at which the size of a growing nucleus is still comparable with the critical size. On the basis of molecular dynamics simulation results for two crystallizing glassy systems, we evaluate the growth laws of the crystalline nuclei and the parameters of the growth kinetics at the temperatures corresponding to deep supercoolings; herein, the statistical treatment of the simulation results is done within the mean-first-passage-time method. It is found for the considered systems at different temperatures that the crystal growth laws rescaled onto the waiting times of the critically-sized nucleus follow the unified dependence, that can simplify significantly theoretical description of the post-nucleation growth of crystalline nuclei. The evaluated size-dependent growth rates are characterized by transition to the steady-state growth regime, which depends on the temperature and occurs in the glassy systems when the size of a growing nucleus becomes two-three times larger than a critical size. It is suggested to consider the temperature dependencies of the crystal growth rate characteristics by using the reduced temperature scale  $\tilde{T}$ . Thus, it is revealed that the scaled values of the crystal growth rate characteristics (namely, the steady-state growth rate and the attachment rate for the critically-sized nucleus) as functions of the reduced temperature  $\tilde{T}$  for glassy systems follow the unified power-law dependencies. This finding is supported by available simulation results; the correspondence with the experimental data for the crystal growth rate in glassy systems at the temperatures near the glass transition is also discussed.

PACS numbers:

## I. INTRODUCTION

A first-order phase transition starts with formation of the nuclei of a new phase. In particular, the nascent liquid droplets represent nuclei of the new (liquid) phase in the case of vapor condensation. Moreover, the bubbles of vapor are such the nuclei at liquid evaporation, while crystallization is initiating through formation of crystalline nuclei. According to classical point of view [1–5], the nucleus of a new phase is capable to demonstrate steady growth, when it reaches a critical size (see Fig. 1). The initial stage of the nucleus growth proceeds through attachment of the particles of the parent phase to the nucleus. When concentration of the growing nuclei become high enough, this growth regime is replaced by the growth through coalescence of the adjacent growing nuclei. The corresponding three processes – the nucleation, the growth by attachment of the particles and the growth through coalescence of growing nuclei – represent general basis of any first-order phase transition [1], whilst the characteristic time scales and rates of the processes are determined by the thermodynamic conditions as well as by inherent features of a system dependent, mainly, on the type of interaction between the structural elements (say, particles) which form a system.

If we restrict our consideration to the crystallization

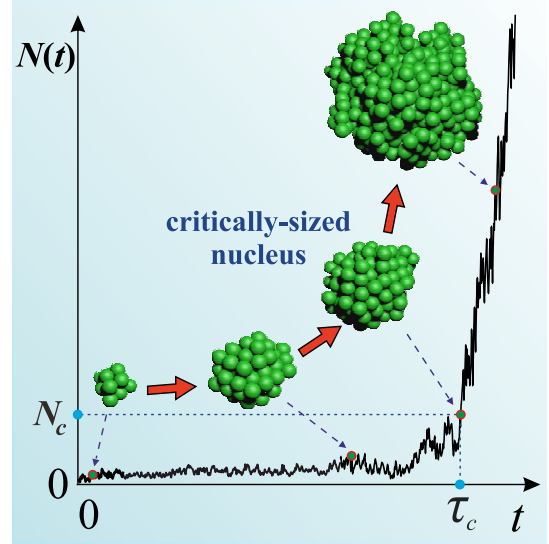


Figure 1: Schematic growth trajectory of the largest crystalline nucleus in a system. Stable growth of a nucleus is possible, when a nucleus reaches the critical size  $N_c$ . Here,  $\tau_c$  is the waiting nucleation time.

kinetics of supercooled liquids, then it is possible for the case to distinguish the inherent features. With increase of the supercooling level, which can be quantified by  $\Delta T/T_m$ , where  $T_m$  is the melting temperature and  $\Delta T = T_m - T$ , the crystal nucleation driving force increases and, thereby, it accelerates structural ordering

---

\*Electronic address: anatolii.mokshin@mail.ru

in the supercooled liquid. On the other hand, with the supercooling increase, the structural transformations is slowing down due to increase of the viscosity. At the supercooling level deep enough to correspond to the glass transition temperature  $T_g$ , the viscosity of a supercooled liquid takes  $\eta \simeq 10^{12}$  Pa·s. As a consequence of high viscosity, the structural transformations in a glass occur so slow, that *overall crystallization* of the glass at a temperature  $T \ll T_g$  is almost unobservable over acceptable time scale, albeit the separate crystal nucleation events still appear [6]. Moreover, extremely small sizes and low concentrations of the nascent crystalline nuclei as well as very low rates of crystal nucleation and of crystal growth complicate the study of the initial regimes of the crystallization in glasses by conventional experimental methods. Thus, if the growth of crystalline clusters in supercooled fluids at low and moderate levels of metastability is sufficiently well-studied subject, then there are still many disputed issues related with the structural ordering in glasses [2, 7–13]. Remarkably, the techniques based on molecular dynamics simulations appear here to be fruitful to elucidate microscopic mechanisms of *initial stages of nucleation and growth processes* for such the thermodynamic conditions where experimental methods have difficulties [1, 14–19].

In recent paper [20], it was reported that the structural ordering in two model glassy systems proceeds through the nucleation mechanism. For both the systems, the nucleation times evaluated as functions of temperature follow the unified scaling law, that was also confirmed by experimental data for the stoichiometric glasses near the glass transition. In the present study, we extend results of Ref. [20] to consideration of the growth kinetics of crystalline nuclei in the glassy systems by focusing mainly on the initial stage of the crystalline nuclei growth, where the non-stationary effects associated with nucleus size fluctuations and with strong size- and time-dependencies of the nucleus growth rate can be very significant. In the study, we apply a statistical treatment of simulation results for the growth kinetics, that is realized, in particular, within the suggested method of inverted averaging of the independent growth trajectories. As a result, the growth law with the characteristics (the growth rate, the growth lag-time, the growth exponent) is defined for each considered thermodynamic state of the systems, and the corresponding theoretical description becomes possible. Since the growth trajectories are monitored directly starting from a nucleation event, then both non-stationary and steady-state growth regimes are accessible for analysis. In addition, the temperature dependencies of the evaluated rate characteristics of crystal growth kinetics as well as their correspondence to the known experimental data are discussed.

## II. NUCLEI GROWTH

### A. General definitions

Let us start with the growth rate of a nucleus, whose size overcame the critical value. This quantity can be expressed in terms of the number of particles  $N$  as

$$v_N = \frac{dN}{dt} \quad (1a)$$

and through the average radius  $R$  as

$$v_R = \frac{dR}{dt}. \quad (1b)$$

Both quantities  $v_N$  and  $v_R$  are positive, when the cluster has a size larger than the critical size, i.e.  $N > N_c$  and  $R > R_c$ . Here,  $N_c$  is the critical value of the number of particles, which form the nucleus, and  $R_c$  is the critical value of the nucleus radius. Within the notations of the Becker-Döring gain-loss theory for the nucleation, the growth rate  $v_N$  is defined as a difference of attachment-rate  $g^+(N)$  and detachment-rate  $g^-(N)$  coefficients, i.e. [21]

$$v_N = g^+(N) - g^-(N). \quad (2)$$

Taking into account the detailed balance condition

$$g^+(N-1)P(N-1) = g^-(N)P(N), \quad (3a)$$

where

$$P(N) = P_0 \exp\left(-\frac{\Delta G(N)}{k_B T}\right) \quad (3b)$$

is an equilibrium cluster distribution, one obtains

$$v_N = g^+(N) - g^+(N-1) \exp\left[-\frac{\Delta G(N-1) - \Delta G(N)}{k_B T}\right], \quad (4)$$

known as growth equation of the Becker-Döring gain-loss theory [21]. Here,  $\Delta G(N)$  is the free energy cost required to form a nucleus of the size  $N$ , and  $k_B$  denotes the Boltzmann constant,  $T$  is the absolute temperature, and  $P_0$  is a pre-exponential factor. The continuous version of this equation has the form [22]

$$v_N = g^+(N) \left\{ 1 - \exp\left[\frac{1}{k_B T} \frac{d\Delta G(N)}{dN}\right] \right\} + \frac{dg^+(N)}{dN} \exp\left[\frac{1}{k_B T} \frac{d\Delta G(N)}{dN}\right]. \quad (5)$$

Moreover, according to the classical nucleation theory the free energy  $\Delta G(N)$  represents the sum of the negative bulk contribution  $-|\Delta\mu|N$  and the positive surface contribution  $\alpha_s N^{2/3}$ , i.e.

$$\Delta G(N) = -|\Delta\mu|N + \alpha_s N^{2/3}, \quad (6)$$

where  $|\Delta\mu|$  is the difference of the chemical potential per phase unite in the melt and the crystal; and  $\alpha_s$  is the temperature-dependent coefficient proportional to the interfacial free energy  $\gamma_s$ . For the spherical cluster one has  $\alpha_s = (36\pi)^{1/3}\gamma_s/\rho_c^{2/3}$  with  $\rho_c$  being the numerical density of the nascent (crystalline) phase. From Eq. (6) one finds

$$\frac{d\Delta G(N)}{dN} = |\Delta\mu| \left[ \left( \frac{N_c}{N} \right)^{1/3} - 1 \right], \quad (7)$$

where

$$N_c = \left( \frac{2}{3} \frac{\alpha_s}{|\Delta\mu|} \right)^3 \quad (8)$$

is the critical cluster size. Inserting Eq. (7) into Eq. (5) one obtains

$$\begin{aligned} v_N = & g^+(N) \left\{ 1 - \exp \left[ \frac{|\Delta\mu|}{k_B T} \left( \left( \frac{N_c}{N} \right)^{1/3} - 1 \right) \right] \right\} \\ & + \frac{dg^+(N)}{dN} \exp \left[ \frac{|\Delta\mu|}{k_B T} \left( \left( \frac{N_c}{N} \right)^{1/3} - 1 \right) \right]. \end{aligned} \quad (9)$$

Note that relation (9) has clear physical meaning. Namely, it indicates that the growth rate  $v_N$  corresponds to the kinetic rate  $g^+(N)$  weighted by thermodynamic factor – the term in curly brackets, which represents the fraction of added particles that is not removed due to the detachment process. Hence, Eqs. (4), (5) and (9) define

the growth rate  $v_N$  of the nucleus, whose size is larger than the critical size  $N_c$ , and, that is important, their application is not restricted by a specific shape of the nucleus or by a supercooling range. At the same time, it might be useful to consider some conditions, which lead to known results and models for the growth rate [23] (in Appendix, see the Zeldovich relation (23) for the growth rate, the Wilson-Frenkel theory with Eqs. (25) and (29), the Turnbull-Fisher model with general relation (33) and the Kelton-Greer extension with Eqs. (35) and (39)). In particular, for the case of weak size-dependence of the attachment rate, growth equation (9) takes the form:

$$v_N = g^+(N) \left\{ 1 - \exp \left[ \frac{|\Delta\mu|}{k_B T} \left( \left( \frac{N_c}{N} \right)^{1/3} - 1 \right) \right] \right\} \quad (10)$$

which represents usually a basis for various growth models [1].

### B. Growth of nucleus of near-critical sizes

Taking into account Eq. (9) and the attachment rate of generally accepted form [see Eq. (43) in Appendix]:

$$g^+(N) = g^+(N_c) \left( \frac{N}{N_c} \right)^{(3-p)/3}, \quad 0 < p \leq 3, \quad (11)$$

one obtain directly

$$v_N = \frac{dN}{dt} = g_{N_c}^+ \left( \frac{N}{N_c} \right)^{\frac{3-p}{3}} \left\{ 1 + \left( \frac{3-p}{3N} - 1 \right) \exp \left[ \frac{|\Delta\mu|}{k_B T} \left( \left( \frac{N_c}{N} \right)^{1/3} - 1 \right) \right] \right\}, \quad 0 < p \leq 3. \quad (12)$$

It is important to stress that Eq. (12) follows directly from definition (2) for the growth rate and no additional conditions were applied to values of the critical size and to metastability level as it is done in the cases of *ad hoc* growth models. This equation as well as the continuity equation for the evolving size distribution of the nuclei and the law of conservation of matter are form the set of equations, which are necessary to be resolved to reproduce kinetics of an arbitrary realistic first-order phase transition [24]. Here,  $g^+(N_c)$  is the attachment rate for the critically-sized nucleus. As known, the exponent  $p$  takes the integer values for well-defined growth models including the ballistic and the diffusion-limited models (the corresponding discussion of the issue can be found in Ref. [23]). If the exponent is  $p = 3$ , then one has the attachment rate independent of nucleus size. For other limit case with  $p = 0$ , the attachment rate changes

with increase of nucleus size according to  $g^+(N) \sim N$ . The mixed growth regimes can also arise with the non-integer values of the parameter  $p$  [25, 26]. This is seen from kinetic growth models (41), (42) and (43) given in Appendix. In particular, it is quite reasonable to expect that non-integer values of the parameter  $p$  will be at growth of a nucleus of near-critical sizes, since there is no clearly defined regime of growth at such sizes, while stochastic effects in the post-nucleation growth are significant. Finding general growth law  $N(t)$ , which will exact solution of Eq. (12) and will be valid for a whole size domain and for different growth regimes, is difficult task. Instead of direct resolving of differential Eq. (12), we apply other method. Namely, the growth law of nucleus of near-critical sizes can be formally defined by the corresponding Taylor series expansion:

$$N(t) = N_c + \left. \frac{dN(t)}{dt} \right|_{t \approx \tau_c} (t - \tau_c) + \frac{1}{2} \left. \frac{d^2 N(t)}{dt^2} \right|_{t \approx \tau_c} (t - \tau_c)^2 + \frac{1}{6} \left. \frac{d^3 N(t)}{dt^3} \right|_{t \approx \tau_c} (t - \tau_c)^3 + \mathcal{O}(|t - \tau_c|^4). \quad (13)$$

Then, from Eqs. (11) and (12) one finds that expansion (13) is approximated in the following way:

$$N(t) = N_c + \sum_{k=1}^3 A_k (t - \tau_c)^k, \quad (14a)$$

with the coefficients

$$A_k \simeq \frac{3-p}{3N_c} \frac{1}{k!} (g_{N_c}^+)^k \left( \frac{\beta |\Delta\mu|}{3N_c} \right)^{k-1}, \quad (14b)$$

$$0 < p \leq 3,$$

where  $g_{N_c}^+ \equiv g^+(N_c)$  and  $\beta = 1/(k_B T)$ . As can be seen from Eqs. (14), nucleus growth defined by Eqs. (14) is represented by the sum of three contributions, according to which the nucleus size  $N(t)$  evolves as  $\sim t$ ,  $\sim t^2$  and  $\sim t^3$ , respectively. The coefficient  $A_1 = (3-p)g_{N_c}^+/(3N_c)$  is the growth factor, which has dimension of an inverse time and takes the meaning of an effective growth rate at initial growth regime, i.e.  $A_1 \equiv \vartheta_c$ . Further, the coefficient  $A_2$  accounts for the growth acceleration effects, whereas the term  $A_3$  quantifies the change of the growth acceleration with time for a nucleus of near-critical sizes. With Eq. (14) and known quantities  $\tau_c$  and  $N_c$ , one can evaluate the attachment rate  $g_{N_c}^+$ , the reduced chemical potential difference  $\beta |\Delta\mu|$  and the growth exponent  $p$  by fit of Eq. (14) to an “experimentally” measured growth law.

### III. SIMULATION DETAILS

We consider the growth of crystalline nuclei in two different glass-formers: the single-component Dzugutov (Dz) system with the potential [27]

$$\begin{aligned} \frac{U_{Dz}(r^*)}{\epsilon} &= C (r^{*-m} - D) \exp\left(\frac{c}{r^* - a}\right) \Theta(a - r^*) \\ &+ D \exp\left(\frac{d}{r^* - b}\right) \Theta(b - r^*), \\ r^* &= r_{ij}/\sigma \end{aligned} \quad (15)$$

and the binary Lennard-Jones (bLJ) system  $A_{80}B_{20}$ , where the particles interact via the potential [20]

$$\begin{aligned} \frac{U_{bLJ}(r_{\alpha\beta}^*)}{\epsilon_{\alpha\beta}} &= 4 [(r_{\alpha\beta}^*)^{-12} - (r_{\alpha\beta}^*)^{-6}], \quad (16) \\ r_{\alpha\beta}^* &= r_{ij}^{\alpha\beta}/\sigma_{\alpha\beta}, \\ \alpha, \beta &\in \{A, B\}. \end{aligned}$$

Numerical values of the parameters for both the potentials are presented in Tab. I. Here,  $r_{ij}$  is the distance between  $i$ -th and  $j$ -th particles,  $\Theta(\dots)$  is the Heaviside step-function. For the case of the bLJ-system with potential (16), the labels  $A$  and  $B$  denote the type of particles, and the semi-empirical (incomplete) Lorentz-Berthelot mixing rules are applied (see Tab. I). The characteristics of the potentials,  $\sigma$  and  $\epsilon$ , set the unit distance and the unit energy, correspondingly, whilst the unit time is  $\tau = \sigma \sqrt{m/\epsilon}$ ; the particles are of the same mass, i.e.  $m = m_A = m_B = 1$  [20].<sup>1</sup>

Table I: Parameters of the Dz-potential (15) and bLJ-potential (16).

Dz						
$C$	$D$	$m$	$a$	$b$	$c$	$d$
5.82	1.28	16	1.87	1.94	1.1	0.27

bLJ					
$\sigma_{\alpha\alpha}$	$\epsilon_{\alpha\alpha}$	$\sigma_{\beta\beta}$	$\epsilon_{\beta\beta}$	$\sigma_{\alpha\beta}$	$\epsilon_{\alpha\beta}$
1.0 $\sigma$	1.0 $\epsilon$	0.8 $\sigma$	0.5 $\epsilon$	0.9 $\sigma$	1.5 $\epsilon$

Simulations with the time step  $\Delta t = 0.005 \tau$  were performed in the  $\mathcal{NPT}$ -ensemble, where the temperature  $T$  and the pressure  $P$  were controlled by the Nosé-Hoover thermostat and barostat [20]. For a single simulation run,  $\mathcal{N} = 6\,912$  particles were included into a cubic simulation cell of the volume  $V = l_x^3$ ,  $l_x = l_y = l_z \simeq 20 \sigma$ , and the periodic boundary conditions are imposed onto all the directions. Glassy samples were generated by fast isobaric cooling with the rate  $dT/dt = 0.001 \epsilon/(k_B \tau)$  of well equilibrated fluid according to algorithm presented in details in Ref. [20]. As a result, glassy samples were prepared at temperatures below the glass-transition temperature  $T_g$  along the isobars with the pressure  $P = 14 \epsilon/\sigma^3$  for the Dz-system and with the pressure  $P = 17 \epsilon/\sigma^3$  for the bLJ-system. The Dz-system at the pressure  $P = 14 \epsilon/\sigma^3$  is characterized by the melting temperature  $T_m \simeq 1.51 \epsilon/k_B$  and the glass transition temperature  $T_g \simeq 0.65 \epsilon/k_B$  at such the cooling rate [28], while for the bLJ-system at the pressure  $P = 17 \epsilon/\sigma^3$  one has

<sup>1</sup> Note that the considered here binary Lennard-Jones system is characterized by different mixing rules in comparison with the Kob-Anderson and Wahnström binary Lennard-Jones systems. Thereby, it differs from these systems, which form very stable glassy states and which do not crystallize over simulation time scales.

the melting temperature  $T_m \simeq 1.65 \epsilon/k_B$  and the glass transition temperature  $T_g \simeq 0.92 \epsilon/k_B$ .

Note that to perform the statistical treatment of the simulation results, more than fifty independent samples were generated for each considered  $(P, T)$ -state of the systems.

Table II: Values of the critical size  $N_c$  and the average waiting time of the critically-sized nucleus  $\tau_c$ .

	$T (\epsilon/k_B)$	$N_c$	$\tau_c (\tau)$
Dz	0.05	$88 \pm 6$	$372 \pm 60$
	0.1	$92 \pm 5$	$340 \pm 55$
	0.15	$96 \pm 5$	$305 \pm 40$
	0.3	$105 \pm 6$	$250 \pm 40$
	0.5	$108 \pm 5$	$220 \pm 30$
bLJ	0.05	$55 \pm 3$	$820 \pm 80$
	0.1	$57 \pm 4$	$800 \pm 75$
	0.2	$58 \pm 4$	$795 \pm 65$
	0.3	$59 \pm 4$	$785 \pm 60$

#### IV. NUCLEATION PARAMETERS AND GROWTH CURVES FROM MOLECULAR DYNAMICS SIMULATION DATA

Classical molecular dynamics simulations allow one to obtain information about positions of all the particles, which generate the system. To identify the nuclei of an ordered phase for an instantaneous configuration of the system we apply the cluster analysis introduced originally in Ref. [29] and based on computation of the local orientational order parameters,  $q_4(i)$ ,  $q_6(i)$ ,  $q_8(i)$ , for each  $i$ th particle [30]. Details of the algorithm are given in Refs. [20, 31]. By means of the cluster analysis we obtain for each  $\alpha$ th simulation run the time-dependent growth trajectory  $N_\alpha(t)$ , which defines the number of particles that belongs to the largest nucleus in the system at time  $t$ . Here,  $\alpha$  is the label of simulation run for the  $(P, T)$ -state. Four growth trajectories  $N(t)$  of the largest nucleus from the independent molecular dynamics simulations are shown in Fig. 2(a). Moreover, from the set of trajectories  $N_\alpha(t)$ , where  $\alpha = 1, 2, 3, \dots, 50$ , for the  $(P, T)$ -state, the curve  $\bar{t}(N)$  is defined, which is known as the mean-first-passage-time curve and which characterizes the average time of the first appearance of a nucleus with given size  $N$ . In accordance with the mean-first-passage-time method [32], the inflection point of this curve gives the critical size  $N_c$  and the average time  $\tau_c$  needed to reach it, i.e.  $\tau_c \equiv \bar{t}(N_c)$ . As an illustration, Fig. 2(c) shows a typical mean-first-passage-time curve derived from the growth trajectories including these given in Fig. 2(a). Further, the inverted mean-first-passage-time curve  $N(\bar{t})$  for sizes  $N \geq N_c$  and times  $t \geq \tau_c$  will reproduce growth law of a nucleus in system [see Fig. 2(b)]. Then, the curve  $N(\bar{t})$  can be used to extract the values of growth parameters or to test a theoretical model of nucleus growth [33].

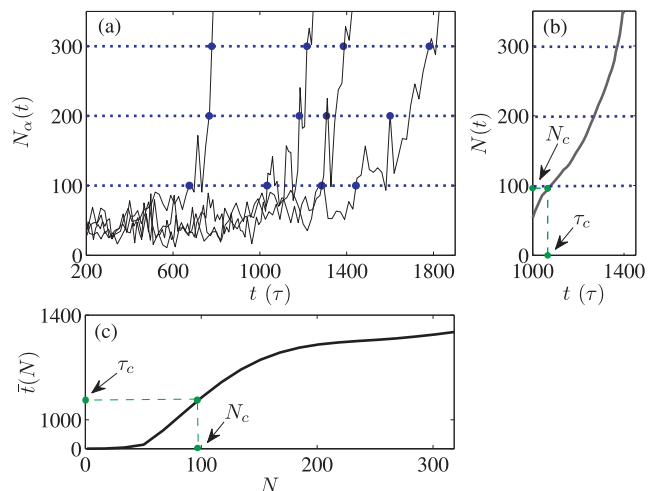


Figure 2: Statistical treatment of the simulation results within the mean-first-passage-time method. (a) Time-dependent growth trajectories  $N_\alpha(t)$  of the largest nucleus extracted from the data of four independent simulation runs ( $\alpha = 1, 2, 3, 4$ ) for the system at a  $(P, T)$ -state. (b) Growth law  $N(t)$  of the largest nucleus recovered by averaging over fifty growth trajectories including these four given on panel (a). (c) Mean-first-passage-time curve defined for the size of the largest nucleus. The inflection point of this curve defines the critical size  $N_c$  and the average waiting time of the critically-sized nucleus  $\tau_c \equiv \bar{t}(N_c)$ .

The attachment rate  $g_{N_c}^+$  can be computed on the basis of the molecular dynamics simulation data by means of the method suggested in Ref. [29]. Namely, the quantity  $g_{N_c}^+$  is defined through the mean-square change of the nucleus size in the neighborhood of the critical size:

$$g_{N_c}^+ = \frac{\langle [N(t) - N_c]^2 \rangle}{2\tau_w}, \quad (17)$$

where  $t \in [\tau_c - \tau_w; \tau_c + \tau_w]$  and  $\tau_w$  is the time window, over which the nucleus evolution is traced<sup>3</sup>. The angle brackets  $\langle \dots \rangle$  means the average over independent growth trajectories  $N(t)$ .

## V. RESULTS

### A. Growth laws

The cluster analysis reveals that the particles of growing clusters are located mainly according to fcc structure, while few amount of the surface particles correspond to hcp structure. This is observed for both the systems at all the considered temperatures. Figure 3 demonstrates,

<sup>3</sup> In this work, the computation of  $g_{N_c}^+$  was done on the basis of the data for the largest crystalline nucleus.

as an example, the crystalline clusters emerging in the Dz- and bLJ-systems and recognized by means of the cluster analysis.

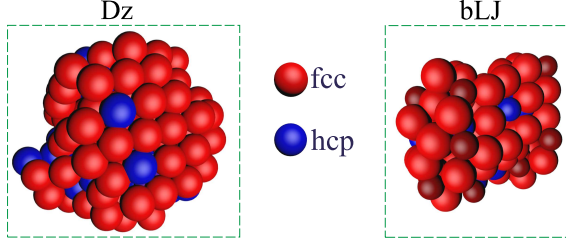


Figure 3: Snapshots of the crystalline clusters arising in the Dz-system at  $T = 0.5 \epsilon/k_B$  and in bLJ-system at  $T = 0.3 \epsilon/k_B$  for which the particles recognized as belonging to fcc and hcp crystalline phases.

The growth curves of the first (largest) crystalline nucleus in the glassy Dz- and bLJ-systems at different temperatures are presented in Fig. 4 (top panel). Here, given results are relevant to the earliest stage of the nucleus growth, where the nucleus size increases threefold. As it was expected, the growth process is slowing down with decrease of the temperature  $T$ . This is evidenced for both the systems by a shift of the growth curves with lower temperatures to the domain of longer times.

On middle panel of Fig. 4, the growth curves are shown in rescaled form, according to which time-scale is expressed in units of the waiting time  $\tau_c$ . Moreover, unit is subtracted from the times in the rescaling in order to relate the start of the nucleus growth with the zeroth time. As a result of the rescaling, the growth curves are collapsed onto a master-curve. The unified behavior of the rescaled growth curves with respect to the temperature  $T$ , which is observed in Fig. 4, indicates that the crystal nucleation and growth processes in the glassy systems could be of the same *kinetic* origin. This means that there are unified mechanisms of the growth kinetics in the glassy systems, and the corresponding theoretical description could be done within a general kinetic model for the growth law. We note that the similar features were observed before for the growth of the crystalline nuclei in a model glassy system under homogeneous shear [34–37] as well as for the droplet growth in supersaturated water vapor [33].

Taking into account that for each the considered  $(P, T)$ -state of both the systems, the attachment rate  $g^+(N_c)$  is determined (will be discussed below), while the critical size  $N_c$  as well as the waiting time  $\tau_c$  are computed by means of the mean-first-passage-time method [20], it becomes possible to fulfill the fit of the growth curves presented in Fig. 4 (middle panel) by Eqs. (14) taking the reduced chemical potential difference  $\beta|\Delta\mu|$  and the growth exponent  $p$  as adjustable

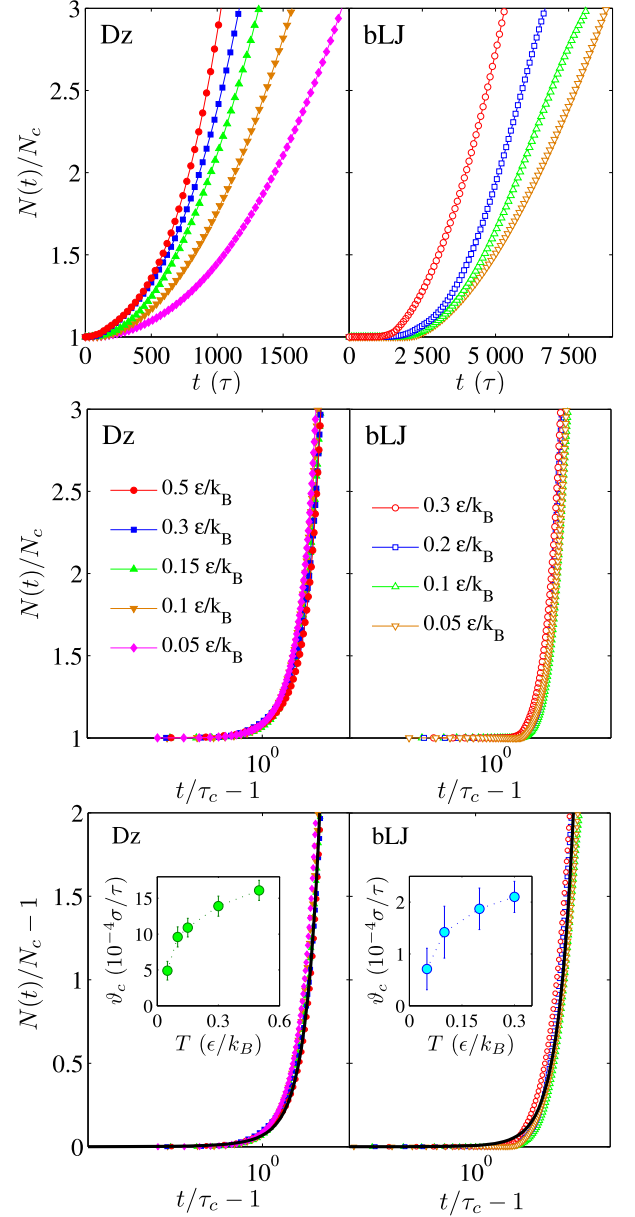


Figure 4: **Top panel:** Growth curves of the crystalline largest nucleus in glassy Dz- and bLJ-systems at different temperatures. Each growth curve is a result of the statistical averaging of the evolution trajectories for the largest nucleus evaluated from the independent simulation runs. For clarity, the nucleus size  $N(t)$  is rescaled onto the critical size  $N_c$ . **Middle panel:** Growth curves rescaled onto the waiting time of the critically sized nucleus  $\tau_c$ . For clarity, the time-axis is taken in a logarithmic scale. **Bottom panel:** (Main) Rescaled growth curves fitted by Eq. (14). Dotted curves correspond to the simulation results; solid curves represent the fit by Eqs. (14). (Insets) Temperature dependencies of the evaluated growth factor  $\vartheta_c$ .



parameters.<sup>1</sup> The values of the nucleation characteristics (the critical size  $N_c$  and the average waiting time of the critically-sized nucleus  $\tau_c$ ) determined by means of the method presented in section IV on the basis of fifty independent trajectories  $N_\alpha(t)$  for each temperature are given in Table II. As can be seen from Fig. 4 (bottom panel), the resulted master-curves of crystal nuclei growth in both the systems are reproducible by growth law (14). Recall that the presented growth curves are resulted from averaging over fifty independent growth trajectories. As follows from our analysis, such the statistics is not sufficient to obtain perfect collapse for all the cases over whole considered time range. Nevertheless, this is quite enough to observe unified behavior of the growth curves as seen from results of Fig. 4. Insignificant deviations the master-curves from growth law (14) are completely covered by small numerical errors of estimated values of the quantities  $\beta|\Delta\mu|$  and  $p$ . We found that the growth exponent  $p$  takes the value  $p = 2.8 \pm 0.15$  for the Dz-system and  $p = 2.99 \pm 0.01$  for the bLJ-system. Note that the exponent  $p$  does not change these values for both the systems over whole the considered temperature range. The growth law with the values of the exponent indicates that the attachment rate is practically independent of the nucleus size,  $g^+(N) \simeq g_{N_c}^+$ , at the earliest stage of the nucleus growth. Note that deviation of values of the parameter  $p$  from integers can be due to the fact that there is no clearly defined regime of nucleus growth at such sizes, while stochastic effects in the post-nucleation growth are significant. Further, we find that the reduced chemical potential  $\beta|\Delta\mu|$  is practically unchanged for the systems within the considered temperature range. Namely, one has the values  $\beta|\Delta\mu| = 0.215 \pm 0.016$  and  $0.167 \pm 0.014$  over the temperature range  $[0.05; 0.5] \epsilon/k_B$  for the case of the Dz-system, and  $\beta|\Delta\mu| = 0.131 \pm 0.013$  and  $0.122 \pm 0.013$  within the temperature range  $[0.05; 0.3] \epsilon/k_B$  for the case of the bLJ-system.

## B. Growth rate

As seen in Fig. 4, some time after a start of the nucleus growth, the steady growth regime is established, where the time-dependent nucleus size is well interpolated by a linear dependence. Since time derivative of a growth curve defines the time-dependent growth rate  $v(t)$  [according to definition (1a)], then the derivative have to approach a constant value  $v^{(st)}$  for the steady-

state growth regime.<sup>2</sup> The growth rate as function of time,  $v(t)$ , was numerically computed for each the considered state of the systems on the basis of the growth trajectories  $N(t)$ , and the size-dependent growth rate  $v_N$  was determined from the available data for  $N(t)$  and  $v(t)$  by simple correspondence of the rates  $v$ 's and the nucleus sizes  $N$ 's at the same time points.

The computed growth rates as functions of the rescaled size  $N/N_c$  for the systems at different temperatures are presented in Fig. 5. As expected, the lower growth rates corresponds to the states with the lower temperatures. One can see from the figure that the growth rate  $v_N$  increases initially with the size  $N$  and then it reaches the steady-state value  $v^{(st)}$  for each considered case. Remarkably, the steady-state growth regime occurs when the cluster size is still comparable with the critical size  $N_c$ . For the glassy Dz-system at the temperatures  $T = [0.05; 0.5] \epsilon/k_B$  the transition into a steady-state growth appears at the cluster size  $N \simeq [2.5; 3]N_c$ , whereas for the glassy bLJ-system at the temperatures  $T = [0.05; 0.3] \epsilon/k_B$  one has the transition at  $N \simeq [1.7; 3]N_c$ . Moreover, the lower temperature  $T$ , the smaller value of the cluster size at which the transition occurs.

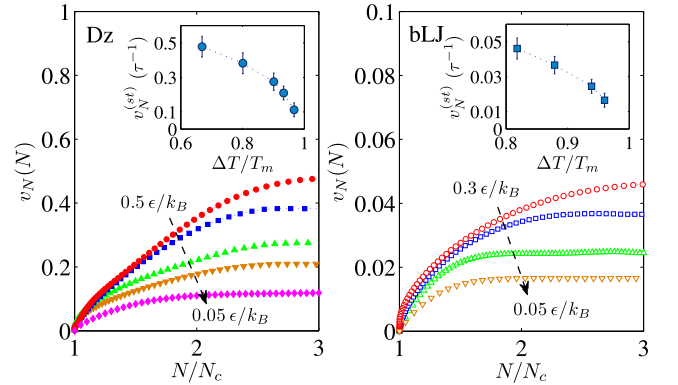


Figure 5: **Main panels:** Growth rate curves  $v_N$  dependent on the crystalline nucleus size for the Dz- and bLJ-systems at different temperatures. **Insets:** Steady-state growth rate  $v_N^{(st)}$  as a function of  $\Delta T/T_m$ . Note that the growth law with Eq. (13) and its time derivative  $dN(t)/dt$  represent, in fact, the parametric equations for  $v_N(N)$ . The values of the steady-state growth rate  $v_N^{(st)}$  were estimated by means of numerical solution of the parametric equations.

The steady-state growth rate  $v_N^{(st)}$  vs. the supercooling level  $\Delta T/T_m$  is shown in insets of Fig. 5. As seen, the growth rate  $v_N^{(st)}$  for both the systems decreases with increase of the supercooling  $\Delta T/T_m$  in such a way that the growth rates are extrapolated to the zeroth values as

<sup>1</sup> As shown previously in Refs. [38, 39], all the particles of a binary system can be considered without division into subtypes at relatively small difference in such the characteristics of a binary system as the partial concentrations, the particle masses and the particle sizes.

<sup>2</sup> Note that the steady-state growth regime means here a case, in which the growth rate becomes independent of time.

we approach  $\Delta T/T_m = 1$  and  $T_0 = 0$  K. The observed temperature dependence of the steady-state growth rate  $v_N^{(st)}$  differ from that appears at *low levels of supercooling*, where the growth rate  $v_N^{(st)}$  is proportional to  $\Delta T/T_m$  [see Eqs. (28), (29) and (40) in Appendix].

As seen from insets of Fig. 5, the temperature dependencies of the steady-state growth rate for both the systems are similar. If such the behavior is of a common physical origin for the levels of supercooling, then the behavior has to be reproducible within a unified scaling relation, where scaled values of the rate characteristic (and of the growth rate) should be taken as a function of the reduced temperature [20]. For the temperature range  $0 < T < T_m$  corresponding to supercooled liquid and glass, it looks to be natural to use  $T/T_m$  or the supercooling  $(T_m - T)/T_m$  as the reduced temperature. However, in this case a reasonable consistency in the scaling can be expected only at the temperatures near melting [6]. Moreover, if one uses the quantity  $T/T_g$  as the reduced temperature, as it is doing, for example, at construction of the scaled structural relaxation time (or of the scaled viscosity) in the Angell-plot [40], then the correspondence in time-dependent values of the rate characteristic for the different systems will be observed in the neighborhood of the glass transition temperature  $T_g$ . Consequently, the temperatures  $\tilde{T} = T/T_m$  or  $\tilde{T} = T/T_g$  cannot be considered as convenient parameters at examination of unified regularities, and a more adaptive scaling scheme is required.

To compare our results as well as available experimental data we apply the method presented in Ref. [20]. Main idea of the method is to display the temperature dependencies of the quantities in the reduced temperature scale  $\tilde{T}$ , where the values of the zeroth temperature  $T_0 = 0$  K, the glass transition temperature  $T_g$  and the melting temperature  $T_m$  are fixed and have same values  $\tilde{T}_0 = 0$ ,  $\tilde{T}_g = 0.5$  and  $\tilde{T}_m = 1$  for all systems. The correspondence between the absolute temperatures  $T$  and the reduced temperatures  $\tilde{T}$  is determined by [20]

$$\tilde{T} = K_1 \left( \frac{T}{T_g} \right) + K_2 \left( \frac{T}{T_g} \right)^2, \quad (18a)$$

with the weight coefficients  $K_1$  and  $K_2$ :

$$K_1 + K_2 = 0.5, \quad (18b)$$

$$K_1 = \left( \frac{0.5 - \frac{T_g^2}{T_m^2}}{1 - \frac{T_g}{T_m}} \right), \quad K_2 = \left( \frac{\frac{T_g}{T_m} - 0.5}{\frac{T_g}{T_m} - 1} \right). \quad (18c)$$

Here, the melting temperature  $T_m$  and the glass transition temperature  $T_g$  are input parameters, which are taken in the absolute units.

Following Ref. [20], we assume that the  $\tilde{T}$ -dependence of the growth rate  $v_R^{(st)}(\tilde{T})$  [and/or  $v_N^{(st)}(\tilde{T})$ ] obeys the

power-law

$$v_R^{(st)}(\tilde{T}) = v_R^{(g)} \left( \frac{\tilde{T}}{\tilde{T}_g} \right)^\chi, \quad (19)$$

where  $\tilde{T}_g = 0.5$  and  $v_R^{(g)}$  is the growth rate of the crystalline nucleus at the temperature  $T_g$ . The exponent  $\chi > 0$  characterizes glass-forming properties of the system. Namely, it takes small values for the case of the systems, which are not capable to retain a disordered phase, and, vice versa, the exponent  $\chi$  must be characterized by high values for the good glass-formers [20]. In this regard it is relevant to mention the recent work of Tang and Harrowell [14], where the maximum in the crystal growth rate is considered as a quantity correlated with the glass-forming ability. Since the maximum of  $v_R^{(st)}$  is defined by the variation of the growth rate with the temperature (with the undercooling), then the exponent  $\chi$  in relation (19) can be considered as a simple measure of the glass-forming ability. The validity of relation (19) is easily tested by mapping the values of the rescaled growth rate into the logarithmic scale as  $(1/\chi) \log_{10}[v_R^{(st)}(\tilde{T})/v_R^{(g)}]$ . In such representation, the parameter  $\chi$  corrects the slope of the data in  $\tilde{T}$ -dependence and the value of  $\chi$  is adjusted so to put the data onto the master-curve

$$\frac{v_R^{(st)}(\tilde{T})}{v_R^{(g)}} = \frac{\tilde{T}}{\tilde{T}_g}. \quad (20)$$

The temperature dependencies of the growth rates evaluated for case of the Dz- and bLJ-systems as well as estimated from molecular dynamics simulations of crystallized single-component LJ-system [41] and tantal [15] and the available experimental data for the crystal growth rates  $v_R^{(st)}$  for  $\text{SiO}_2$  [42],  $\text{PbO} \cdot \text{SiO}_2$  [42],  $\text{Li}_2\text{O} \cdot 2\text{SiO}_2$  [6],  $\text{Li}_2\text{O} \cdot 3\text{SiO}_2$  [43],  $\text{CaO} \cdot \text{MgO} \cdot 2\text{SiO}_2$  [44],  $2\text{MgO} \cdot 2\text{Al}_2\text{O}_3 \cdot 5\text{SiO}_2$  [44] are given in the same Fig. 6. The defined values of the parameter  $\chi$  as well as the values of the parameter  $v_R^{(g)}$  for the considered systems are presented in Tab. III.

As seen from Fig. 6, the growth rates for all the systems follow the master-curve (20) for the temperatures  $\tilde{T}$  near and below the glass transition temperature  $\tilde{T}_g = 0.5$ . Numerical values of the parameters  $\chi$  and  $v_R^{(g)}$  are given in Tab. III. This directly indicates that behavior of the growth rate  $v_R^{(st)}(\tilde{T})$  for the temperature range,  $\tilde{T} \leq 0.5$ , is reproducible by the power-law and relation (19) is unified for the  $\tilde{T}$ -dependent growth rates of the systems. This result is consistent with the findings of Ref. [20], where it was demonstrated that the scaled crystal nucleation time  $\tau_1$  in glassy systems as a function of the reduced temperature  $\tilde{T}$  follows the unified power-law dependence  $\tau_1 \sim (1/\tilde{T})^\gamma$ . In addition, the power-law temperature dependence of the structural relaxation time  $\tau_\alpha \sim (1/\tilde{T})^\gamma$  generalizes the Avramov-Milchev model for the viscosity [20], while the exponent  $\gamma$  is related with the



Table III: The melting temperature  $T_m$ , the glass transition temperature  $T_g$ , the steady-state growth rate  $v_R^{(g)}$  at the transition temperature  $T_g$ , the exponent  $\chi$  found from Eq. (19), the attachment rate  $g_{N_c}^{(g)}$  at the glass transition temperature  $T_g$ , the exponent  $\varsigma$  evaluated from fit of Eq. (21) to the simulation results.

	System	$T_m$	$T_g$	$v_R^{(g)}$	$\chi$	$g_{N_c}^{(g)}$	$\varsigma$
	Dz (at $P = 14\varepsilon/\sigma^3$ )	$1.51 \varepsilon/k_B$	$0.65 \varepsilon/k_B$	$(23.8 \pm 2.7) \cdot 10^{-4} \sigma/\tau$	$0.37 \pm 0.06$	$(13.9 \pm 1.6) \cdot \tau^{-1}$	$0.31 \pm 0.04$
	bLJ (at $P = 17\varepsilon/\sigma^3$ )	$1.65 \varepsilon/k_B$	$0.92 \varepsilon/k_B$	$(4.7 \pm 0.7) \cdot 10^{-4} \sigma/\tau$	$0.41 \pm 0.07$	$(13.1 \pm 1.5) \cdot \tau^{-1}$	$0.58 \pm 0.06$
[41]	LJ	$0.62 \varepsilon/k_B$	$0.4 \varepsilon/k_B$	$0.41 \pm 0.05 \sigma/\tau$	$0.39 \pm 0.07$	—	—
[15]	Ta	3 290 K	1 650 K	$41.5 \pm 4 \text{ m/s}$	$3.5 \pm 0.6$	—	—
[42]	SiO <sub>2</sub>	2 000 K	1 450 K	$(1.1 \pm 0.2) \cdot 10^{-12} \text{ m/s}$	$12.6 \pm 1.4$	—	—
[42]	PbO·SiO <sub>2</sub>	1 037 K	673 K	$(1.5 \pm 0.2) \cdot 10^{-11} \text{ m/s}$	$22.6 \pm 1.5$	—	—
[6]	Li <sub>2</sub> O·2SiO <sub>2</sub>	1 306 K	727 K	$(2.2 \pm 0.4) \cdot 10^{-12} \text{ m/s}$	$49.2 \pm 4.5$	—	—
[43]	Li <sub>2</sub> O·3SiO <sub>2</sub>	1 306 K	734 K	$(1.1 \pm 0.3) \cdot 10^{-11} \text{ m/s}$	$34.5 \pm 2.5$	—	—
[44]	CaO·MgO·2SiO <sub>2</sub>	1 664 K	993 K	$(9.4 \pm 1.2) \cdot 10^{-14} \text{ m/s}$	$49.8 \pm 4.8$	—	—
[44]	2MgO·2Al <sub>2</sub> O <sub>3</sub> · 5SiO <sub>2</sub>	1 740 K	1 088 K	$(3.9 \pm 0.8) \cdot 10^{-12} \text{ m/s}$	$53.2 \pm 6.2$	—	—

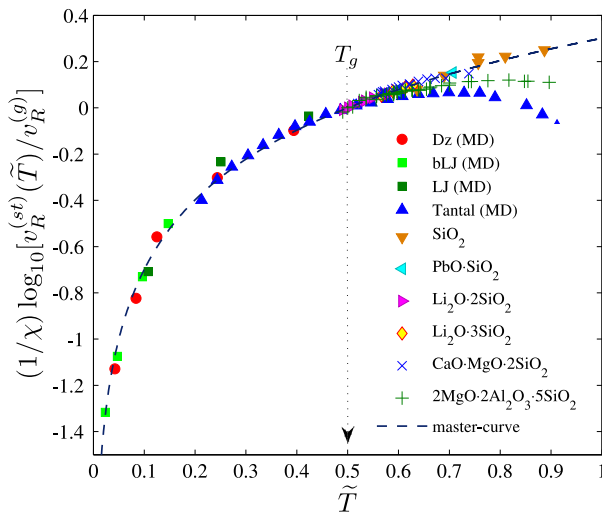


Figure 6: Scaled growth rates  $v_R^{(st)}$  vs. reduced temperature  $\tilde{T}$ . Such the plot allows one to compare the simulation results for the glassy Dz- and bLJ-systems, the simulation results for the supercooled LJ-system [41] and tantal [15], the experimental data for the supercooled SiO<sub>2</sub> [42], PbO·SiO<sub>2</sub> [42], Li<sub>2</sub>O·2SiO<sub>2</sub> [6], Li<sub>2</sub>O·3SiO<sub>2</sub> [43], CaO·MgO·2SiO<sub>2</sub> [44] and 2MgO·2Al<sub>2</sub>O<sub>3</sub> · 5SiO<sub>2</sub> [44]. The dashed line reproduces the master-curve (20). Arrow indicates the scaled glass transition temperature  $\tilde{T}_g = 0.5$ . For the glassy Dz- and bLJ-systems, values of  $v_R^{(g)}$  were defined by extrapolation of the data  $v_R^{(st)}(\tilde{T})$  to the temperature  $\tilde{T}_g = 0.5$ . Values of the parameters  $\chi$  and  $v_R^{(g)}$  are given in Tab. III.

fragility index  $m$ . Therefore, it quite reasonable to anticipate that such the temperature dependence is generic for the rate characteristics of structural transformations in glasses, where the inherent kinetics is dominant over thermodynamic aspects. This is differ from how nucleation and growth proceed at the low levels of supercooling, where impact of the thermodynamic contributions on the values of the rates is significant and where the growth rate  $v_R^{(st)}$  increases with increase of supercooling [3]. Thus,

the character of the  $\tilde{T}$ -dependent growth rates for the low supercoolings diverges from the  $\tilde{T}$ -dependence specified by Eq. (19). As can be seen in Fig. 6, the behavior of the curve  $v_R^{(st)}(\tilde{T})$  for the systems starts to be different as the temperature  $\tilde{T}$  approaches the melting point  $\tilde{T}_m = 1$ , where the growth rate  $v_R^{(st)}(\tilde{T}_m)$  is equal to zero for any system.

### C. Attachment rate

Since the growth kinetics depends directly on the attachment rate,  $g_N^+ \equiv g^+(N)$  [see Eq. (9)], therefore, it is important to consider how the quantity  $g_N^+$  behaves with the temperature variation, that can be done with the term  $g_{N_c}^+$ , which is the attachment rate for the critically-sized nucleus. We recall here that some theoretical models of the growth kinetics (e.g., the Turnbull-Fisher model with relation (33) as well as the Kelton-Greer extension with relation (38), see Appendix) utilize the quantity  $g_{N_c}^+$  instead of the size dependent  $g_N^+$ .

The values of the quantity  $g_{N_c}^+$  for both the systems are given in Fig. 7(a), where the temperature is plotted into the reduced scale,  $\tilde{T}$ . As can be seen, the quantity  $g_{N_c}^+$  decreases with the decrease of the temperature. Nevertheless, the attachment rate as well as the growth rate take the finite values for the systems even at the deep levels of supercooling, and are still detectable over a simulation time scale. Hence, even insignificant displacements of the particles may result in structural transformations in high-density glassy systems, where the particles interact through an isotropic potential [20, 45, 46].

By analogy with results for the steady-state growth rate (see Fig. 6), the scaled attachment rate versus the reduced temperature  $\tilde{T}$  is presented in Fig. 7(b). Here, the parameter  $g_{N_c}^{(g)}$  is the attachment rate at the glass transition temperature  $\tilde{T}_g = 0.5$ , and its numerical values for the systems are estimated by extrapolation of the attachment rate  $g_{N_c}^+(\tilde{T})$  to the temperature domain

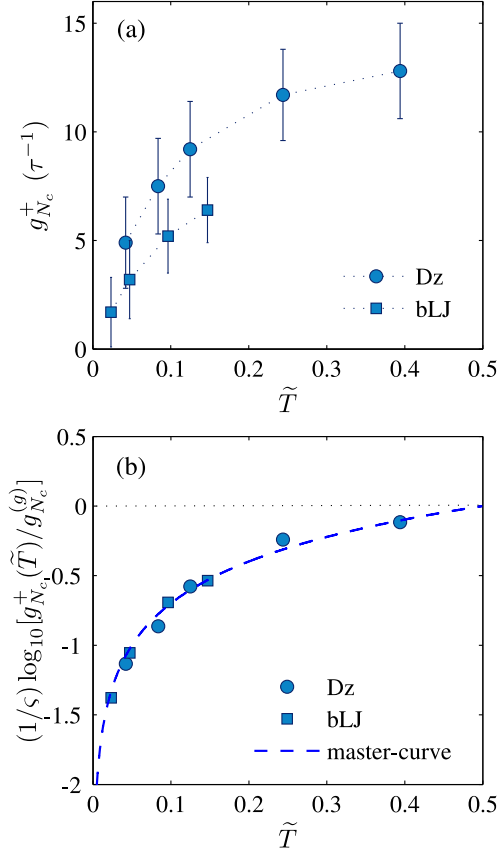


Figure 7: (a) Attachment rate for the critically-sized nucleus  $g_{N_c}^+$  as a function of the reduced temperature  $\tilde{T}$  for the Dz-system and for the bLJ-system. (b) Scaled attachment rate  $(1/\varsigma) \log_{10}[g_{N_c}^+(\tilde{T})/g_{N_c}^{(g)}]$  versus the reduced temperature  $\tilde{T}$ . The values of the attachment rate  $g_{N_c}^{(g)}$  for the systems are evaluated by extrapolation data  $g_{N_c}^+(\tilde{T})$  to the glass transition temperature  $\tilde{T}_g$ . The dashed line corresponds to the master-curve  $g_{N_c}^+(\tilde{T})/g_{N_c}^{(g)} = \tilde{T}/\tilde{T}_g$ . Values of the exponent  $\varsigma$  and the quantity  $g_{N_c}^{(g)}$  are given in Tab. III.

near  $\tilde{T}_g$ . The exponent  $\varsigma$  characterizes how the attachment rate changes with the temperature, that is similar to physical meaning of the exponent  $\chi$ . At the construction of Fig. 7(b), the exponent  $\varsigma$  is taken as adjustable parameter, which corrects the slope of a curve; while the quantity  $g_{N_c}^{(g)}$  is defined in a way to guarantee the zeroth value of  $(1/\varsigma) \log_{10}[g_{N_c}^+(\tilde{T})/g_{N_c}^{(g)}]$  at the glass transition temperature  $\tilde{T}_g = 0.5$ . The estimated values of the quantities  $g_{N_c}^{(g)}$  and  $\varsigma$  are given in Tab. III. It is seen from Fig. 7(b) that the  $\tilde{T}$ -dependencies of the obtained attachment rate  $g_{N_c}^+$  for both the glassy systems are well reproduced by the power-law

$$g_{N_c}^+(\tilde{T}) = g_{N_c}^{(g)} \left( \frac{\tilde{T}}{\tilde{T}_g} \right)^\varsigma. \quad (21)$$

[We recall that the glass transition temperature is  $\tilde{T}_g = 0.5$ ].

Remarkably, the exponent  $\varsigma$  takes values close to values of the exponent  $\chi$  characterizing the growth kinetics. This is not surprising, since the growth and attachment rates,  $v_N$  and  $g_{N_c}^+$ , are expected to be significantly correlated at the deep levels of supercooling. Taking into account the defined values of  $g_{N_c}^{(g)}$  we deduce that the attachment rate decreases by two times over the temperature range from  $T_g = 0.65 \text{ } \epsilon/k_B$  to  $T = 0.05 \text{ } \epsilon/k_B$  for the Dz-system and by 4.4 times over the temperature range from  $T_g = 0.92 \text{ } \epsilon/k_B$  to  $T = 0.05 \text{ } \epsilon/k_B$  for the bLJ-system.

## VI. DISCUSSION

Traditional experiments on crystal growth are capable to probe crystalline nuclei within micron size range [21], and the theoretical models for the growth kinetics are required to extrapolate the experimental data into the domain of smaller sizes, where the crystal growth initiated, and to recover overall picture of the nucleation-growth process (see, for example, Refs. [23, 47]). In the given study, we apply an opposite handling. On the basis of simulation data for model glassy systems at different temperatures, the crystal growth is directly restored starting from a nucleation event. This provides a possibility to define the time-dependent crystal growth law as well as to evaluate a crystal growth rate characteristics as size- and temperature-dependent terms.

Statistical treatment of the characteristics of growth kinetics is realized in this study as follows. The growth law is defined by means of the mean-first-passage-time method [31, 33], in which an waiting time scale sets in accordance to the certain size  $N$ . As a result, one can estimate the growth law  $N(t)$  with  $N \geq N_c$  on the basis of the independent growth trajectories for the case, when the direct averaging  $N(t) = \sum N_\alpha(t)$  does not work, because the nucleation time  $\tau_c$  can take a value from a range larger than the characteristic time scale of crystal growth [see Fig. 2(a)]. Within the statistical treatment, the nucleation and growth rate parameters are definable within a common method utilizing the time-dependent growth trajectories resulted from independent experiments or molecular dynamics simulations.

The analysis reveals that an envelope of the nuclei at the initial growth stage is reproduced well by a sphere [20], while the crystalline faces of the nuclei are not well-defined at the stage [48]. In the case, the average nucleus radius coincides with the proper nucleus radius; and one can directly relate the size parameters – the number of particles enclosed in a nucleus  $N$  and the nucleus radius  $R$ . This allows one to carry out reasonably the treatment of the results by means of the so-called “mean radius approaches” [49]. The results obtained in the study reveal that the size of crystalline nuclei in the considered glassy systems evolves with time

at post-nucleation stage according to dependence, which is an approximate solution of the growth equation. Such the character of the growth of nascent crystalline nuclei holds over temperature range. As a result, the growth law can be represented in a unified form with the scaled parameters – the time  $t/\tau_c$  and the size  $N/N_c$ . We stress that such the character of the growth law is consistent with the limit solution of growth equation (12), as well as with the theoretical suggestions (see p. 378 in Ref. [1]) and with previous simulation results [20, 33, 50].

The growth rate at initial growth stage depends strongly on the nucleus size. Nevertheless, at high levels of supercooling considered in the study, transition into the steady-state growth regime arises, when the nucleus size increases in two-three times in respect to a critical size. Notable, the nucleus size  $R$  equal to  $2R_c$  is also mentioned by Langer (p. 14 in Ref. [51]) and is related assumedly with a maximum of growth rate  $v_R$  arisen in the pre-dendritic stage of crystal growth. Hence, the crystalline growth in glasses can be characterized by a single value of the growth rate  $v^{(st)}$  over an extended size range, that simplifies considerably a theoretical description of crystallization kinetics in the systems [2, 3]. Further, according to Eq. (12), the size-dependent growth rate  $v_N$  is defined by the three input quantities: the attachment rate  $g^+(N)$ , the critical size  $N_c$  and the reduced difference of the chemical potential  $|\Delta\mu|/k_B T$ . Here-with, the known theoretical models (see Appendix) are derived from the equation by an approximation for the  $N$ -dependent attachment rate  $g^+(N)$  [as is done, for example, for the pure kinetic models and for kinetic extension of the Turnbull-Fisher model, see Appendix] and/or by considering the system at specific thermodynamic conditions with the given ratios  $|\Delta\mu|/k_B T$  and  $N_c/N$  [as in the Wilson-Frenkel theory [52, 53], see Appendix]. In the present study, consideration of the growth kinetics was directly done on the basis of a primary equation of growth kinetics, i.e. Eq. (12).

According to classical view on the nucleation-growth process [1], the temperature dependence of the growth rate is characterized by a maximum, which appears due to the features in the  $T$ -dependence of the kinetic rate coefficient  $g^+(N)$  and the thermodynamic factor – the expression in curly brackets in Eq. (9), for example. Hence, with decrease of the temperature, the first quantity also decreases, whereas the second term increases. In the given study, we focus on the crystalline nuclei growth in glasses at deep levels of supercooling. At such the thermodynamic conditions, the steady-state growth rate  $v^{(st)}$  is defined mainly by the kinetic term  $g^+(N)$  and, thereby, it increases with the temperature  $T$ , that is opposite to well-known behavior of the growth rate observable experimentally in the systems at low and moderate levels of supercooling [42–44].

General patterns in the temperature dependencies of the growth rate detectable for various crystallizing systems [42, 44] indicates that a unified theoretical description of the growth rate as a function of the tempera-

ture as well as direct comparison of the experimental data for the systems by means of scaling relations are possible. As an attempt to do such the comparison, one can mention the corresponding part in Langer’s review [51] (Fig. 15 on p. 19 and its discussion), where the growth rates measured for ice and succinonitrile are compared with the Ivantsov relation. In particular, it follows from Fig. 15 given in Ref. [51] that the dimensionless growth rate as a function of dimensionless undercooling presented in double-logarithmic plot is well interpolated by a power-law dependence. In this work, we extend the idea of a unified description of the nucleation-growth kinetics [40, 54, 55], that is realized here on the basis of the reduced temperature  $\tilde{T}$ -scale concept [20]. Note that the reduced temperature  $\tilde{T}$ -scale differs from such the dimensionless temperatures applying usually to characterize the thermodynamic states of supercooled liquids and glasses as the undercooling  $\Delta T/T_m$  (see Ref. [56]), or the dimensionless temperatures  $T/T_m$  and  $T/T_g$  (see Ref. [40, 57]). Namely, the  $\tilde{T}$ -scale ranks the temperature range  $0 \leq T \leq T_m$  uniformly for supercooled systems, and, thereby, this allows one to compare the temperature dependent characteristics of the systems, whose the glass-forming abilities differs significantly. By means of this approach, we found that the growth rates extracted from simulations and experimental data for the different systems and plotted as a function of  $\tilde{T}$  in the temperature range  $0 < T \leq T_g$  approximate the power-law dependence with the exponent, which is using as fitting parameter and could be using for numerical estimate of the glass-forming ability of a system [14]. Finally, the attachment rate evaluated on the basis of simulation data and presented as a function of the reduced temperature  $\tilde{T}$  follows also the power-law dependence, which is correlated with the scaling law found before for crystal nucleation times in the systems [20].

Divergence of the growth rate values and their deviation from the universal power-law at the temperatures  $T_g < T < T_m$  is not surprising. At low levels of supercooling, the thermodynamic properties have main impact on the nucleation-growth processes. This is reproducible, in particular, within the Wilson-Frenkel theory (see Eqs. (27) and (29) in Appendix) and the Turnbull-Fisher model (see Eq. (39) in Appendix). Here, the growth rate as well as the nucleation rate are increasing with supercooling increase till the system temperature  $T$  will not be comparable with the glass transition temperature (i.e.  $T \leq T_g$ ), where the nucleation and growth rates take the highest values. With further increase of supercooling, the slowing down of the system kinetics is resulted into decrease of all the transition rate characteristics (namely, the nucleation, growth and attachment rates). Therefore, expectedly, these rates can be correlated as functions of the temperature  $T$  at the range  $0 < T \leq T_g$ . This is supported by simulation results of this study. So, taking the reduced chemical potential  $|\Delta\mu|/(k_B T) \sim 0.19 \pm 0.03$  and the cluster size  $N \geq 3N_c$ ,

at which the steady-state growth rate appears for the Dz-system, one obtains that the exponential function in growth equation (12) becomes approximately equal to unity, whereas  $v_N^{(st)} \sim g_{N_c}^+$  and, consequently, the thermodynamic impact to the growth process is insignificant for the considered temperature range  $0 < T < T_g$ .

Finally, the nucleation-growth rate characteristics and, in particular, the kinetic coefficient  $g_{N_c}^+$  are associated with the mobility of particles and, thereby, with the diffusion (as it is for  $g_{N_c}^+$  in Kelton-Greer model, for example; Eq. (34) in Appendix) as well as with the viscosity (see, for example, the principal equation of the kinetic ballistic model, Eq. (41) in Appendix). In this connection, the unified scenarios in temperature dependencies of the growth and attachment rates presented in this paper provide new important insight into the possibility to develop a general model of viscosity suitable to all supercooled liquids regardless of such the peculiarities as fragility, bonding and particles interaction type [58].

## VII. CONCLUSIONS

The main results of this study are the following:

(i) It is shown that the growth law of nucleus of near-critical sizes can be represented as the cubic polynomial with the coefficients dependent on the critical size, the attachment rate, the chemical potential difference and the growth exponent – i.e. all the quantities incoming into original growth equation. The growth law model is applied to evaluate crystal nuclei data derived from molecular dynamics simulations for two different crystallizing glassy systems at temperatures below  $T_g$  via the mean-first-passage-time analysis.

(ii) It is found that the crystal growth laws of the systems follow the unified time-dependence, where the growth exponent is constant for each the system over whole the considered temperature range.

(iii) The steady-state growth regime, where the growth rate is independent of the cluster size, occurs when the size of growing crystalline nucleus in a glassy system becomes two-three times larger than a critical size.

(iv) The results provide evidence that the rate characteristics of the crystal growth process as temperature dependent quantities are reproducible within unified scaling relations. This finding is supported for the steady-state growth rate and the attachment rate. In particular, values of the reduced steady-state growth rate taken from simulation results and experimental data for different systems and plotted *vs.* the scaled temperature  $\tilde{T}$  are collapsed onto a single line for the temperatures below  $T_g$ . In a similar matter, the reduced attachments rates evaluated for the crystallizing glassy systems and considered as functions of the reduced temperature  $\tilde{T}$  follow the unified power-law dependence.

## Appendix

### Zeldovich relation

For a metastable system being at the low levels of supercooling one can consider the dimensionless term

$$\frac{1}{k_B T} \frac{d\Delta G(N)}{dN} \quad (22)$$

as a term taking small values less than unity. As a result, Eq. (5) simplifies to the well known Zeldovich relation for the growth rate:

$$v_N = -\frac{g^+(N)}{k_B T} \frac{d\Delta G(N)}{dN}. \quad (23)$$

Zeldovich's relation (23) takes into account the fact that the growth rate is resulted from both the thermodynamic and pure kinetic contributions,  $d\Delta G(N)/dN$  and  $g^+(N)$ , while their product defines completely the temperature dependence as well as the size dependence of the growth rate. Nevertheless, the aforementioned condition imposed on the thermodynamic term in Eq. (5) restricts application of the Zeldovich relation (23) to a system being at specific thermodynamic conditions.

### Growth rate within the Wilson-Frenkel theory

For the case, when

$$\left(\frac{N_c}{N}\right)^{1/3} \ll 1, \quad (24)$$

that can be realized in the macroscopic limit, i.e. at the late stage of the growth of a solitary cluster or for growing crystalline slab, Eq. (9) can be rewritten as

$$v_N = g^+(N) \left\{ 1 - \exp \left[ -\frac{|\Delta\mu|}{k_B T} \right] \right\}. \quad (25)$$

For low and relatively moderate levels of supercooling, i.e. for insignificant deviations from equilibrium, the next condition is satisfied:

$$\frac{|\Delta\mu|}{k_B T} \ll 1. \quad (26)$$

Then, Eq. (25) takes the form [52, 53]

$$v_N \simeq g^+(N) \frac{|\Delta\mu|}{k_B T}. \quad (27)$$

Taking into account the thermodynamic identity

$$\frac{\Delta\mu}{k_B T} = \frac{l}{T_m} \frac{\Delta T}{k_B T} = \Delta S \frac{\Delta T}{k_B T}, \quad (28)$$

one comes to the known result, according to which the growth rate  $v_N$  within the Wilson-Frenkel theory [52,

53, 59] is proportional to the supercooling  $\Delta T = T_m - T$ . Here,  $l$  is the latent heat of the transition and  $\Delta S$  is the entropy change between the crystalline and the liquid phases. This allows one to rewrite Eq. (27)

$$v_N = k^{WF} \Delta T, \quad (29)$$

where  $k^{WF}$  being the so-called interface kinetic coefficient.

As follows from the classical nucleation theory, since the chemical potential difference  $|\Delta\mu|$  is inversely proportional to the critical size  $N_c$  [see Eq. (8)], then condition (26) corresponds to the large values of the critical size, that indicates on the correspondence of Eq. (27) to the macroscopic growth rate.

### Turnbull-Fisher model and its kinetic extension

The Turnbull-Fisher model was specially adopted to describe the crystal nucleation and growth in glasses [60]. The model was extensively studied by Kelton et al. [4] and Greer et al. [61].

The structural transformations in glasses are driven rather by kinetic than thermodynamic contribution. This means that the crystal growth in a glass is largely defined by the diffusive processes. In this model it is assumed that the coefficient  $g^+(N)$  can be taken in the form

$$g^+(N) \sim \exp \left[ -\frac{\Delta G(N+1) - \Delta G(N)}{2k_B T} \right]. \quad (30)$$

Inserting Eq. (30) into Eq. (4) by analogy with Eq. (5) one obtains

$$\begin{aligned} v_N &\sim \exp \left[ -\frac{1}{2k_B T} \frac{d\Delta G(N)}{dN} \right] - \exp \left[ \frac{1}{2k_B T} \frac{d\Delta G(N)}{dN} \right] \\ &\sim 2 \sinh \left[ -\frac{1}{2k_B T} \frac{d\Delta G(N)}{dN} \right]. \end{aligned}$$

Then, taking into account Eq. (7) one obtains the growth rate

$$v_N \sim 2 \sinh \left\{ \frac{|\Delta\mu|}{2k_B T} \left[ 1 - \left( \frac{N_c}{N} \right)^{1/3} \right] \right\}. \quad (32)$$

As a result, expression for the Turnbull-Fisher cluster-size-dependent growth rate can be written as

$$\begin{aligned} v_N &= 2g^+(N_c) \left( \frac{N}{N_c} \right)^{2/3} \\ &\times \sinh \left\{ \frac{|\Delta\mu|}{2k_B T} \left[ 1 - \left( \frac{N_c}{N} \right)^{1/3} \right] \right\}, \end{aligned} \quad (33)$$

The Turnbull-Fisher model has been later extended by Kelton and Greer. Namely, Kelton and Greer [62] expressed the coefficient,  $g^+(N_c) \equiv g_{N_c}^+$ , in terms of the ordinary diffusion  $D$  as following

$$g^+(N_c) = 24 \frac{D}{\lambda^2} N_c^{2/3}, \quad (34)$$

where  $\lambda$  is the atomic jump distance. As a result, Eq. (33) takes the form

$$\begin{aligned} v_N &= 48 \frac{D}{\lambda^2} N^{2/3} \\ &\times \sinh \left\{ \frac{|\Delta\mu|}{2k_B T} \left[ 1 - \left( \frac{N_c}{N} \right)^{1/3} \right] \right\}. \end{aligned} \quad (35)$$

For the growth at macroscopic conditions, when the size of the growing cluster is much larger than the critical size  $N_c$ , Eqs. (33) and (35) take the forms,

$$v_N = 2g^+(N_c) \left( \frac{N}{N_c} \right)^{2/3} \sinh \left\{ \frac{|\Delta\mu|}{2k_B T} \right\} \quad (36)$$

and

$$v_N = 48 \frac{D}{\lambda^2} N^{2/3} \sinh \left\{ \frac{|\Delta\mu|}{2k_B T} \right\} \quad (37)$$

respectively.

It is easy to verify that at low levels of supercooling Eqs. (36) and (37) are simplified to the next corresponding relations

$$v_N = g^+(N_c) \left( \frac{N}{N_c} \right)^{2/3} \frac{|\Delta\mu|}{k_B T} \quad (38)$$

and

$$v_N = 24 \frac{D}{\lambda^2} N^{2/3} \frac{|\Delta\mu|}{k_B T}. \quad (39)$$

In Eqs. (38) and (39) the contribution responsible for to reproduce the thermodynamic aspect of cluster growth remains the same, since the Kelton-Greer extension concerns only the kinetic contribution of the Turnbull-Fisher model.

Further, taking into account equality (28), one can see that Eqs. (38) and (39) yield the same linear dependence of the macroscopic growth rate upon the supercooling, i.e.  $v_N \propto \Delta T$ ,

$$\begin{aligned} v_N &\propto \frac{|\Delta\mu|}{k_B T} \\ &\propto \frac{l}{T_m} \frac{\Delta T}{k_B T} \\ &\propto \Delta S \frac{\Delta T}{k_B T}, \end{aligned} \quad (40)$$

which is the same with Eq. (29) derived within the Wilson-Frenkel theory.

### Kinetic models

There are some pure kinetic growth models, which are focused rather upon the mechanisms of mass exchange between the cluster and the mother phase [23]. Hence,

the  $N^{2/3}$ -dependence for the coefficient  $g^+(N)$  is suggested in the so-called ballistic model [63]:

$$g^+(N) = b \frac{k_B T}{\eta \lambda^3} N^{2/3}, \quad (41)$$

where  $\eta$  is the viscosity, and  $b$  is a numerical constant. Since for the three-dimensional growth one has  $dR/dt \propto N^{-2/3} dN/dt$ , then the ballistic model with Eq. (41) correspond to the rate  $g^+(N)$ , which is actually independent of the radius of the cluster, but depends on the properties of the mother phase. As it was discussed in Ref. [63], such the scenario is appropriate, in particular, for the case of the fluid droplet growth in a supersaturated vapor.

Further, at the Ostwald ripening regimes of the growth kinetics other situations appear [26, 64, 65], where the rate  $g^+(N)$  has the size-dependence of the form:

$$g^+(N) \propto N^{1/3} \quad (42a)$$

and the rate  $g^+(N)$  can be even independent of the size:

$$g^+(N) = \text{const.} \quad (42b)$$

As it is seen, relations (41), (42a) and (42b) can be generalized into the power-law dependence [21, 23]

$$g^+(N) \propto N^{(3-p)/3}, \quad (43)$$

with  $0 < p \leq 3$ , where the integer values of the exponent, i.e.  $p = 1, 2, 3$ , correspond to the models (41), (42a) and (42b), respectively.

## Acknowledgments

The authors thank E. Zanotto, D. Kashchiev, V. N. Ryzhov, V. V. Brazhkin for motivating discussions. The work is supported in part by the grant MD-5792.2016.2 (support for young scientists in RF) and by the project of state assignment of KFU in the sphere of scientific activities.

- 
- [1] D. Kashchiev, *Nucleation: Basic Theory with Applications*, Butterworth Heinemann, Oxford U.K., 2000.
  - [2] V. P. Skripov, *Metastable Liquids*, Wiley, New-York, 1974.
  - [3] P. G. Debenedetti, *Metastable Liquids. Concepts and Principles*, Princeton U.P., Princeton, 1996.
  - [4] K. F. Kelton, A. L. Greer and C. B. Thompson, *J. Chem. Phys.*, 1983, **79**, 6261-6276.
  - [5] V. I. Kalikmanov, *Nucleation Theory*, Lecture Notes in Physics, Springer, New York, 2012.
  - [6] V. M. Fokin, N. S. Yuritsin, O. V. Potapov, B. S. Shakhmatkin, N. M. Vedisheva, V. L. Ugolkov, A. G. Cherepova, *Russ. J. Phys. Chem. A*, 2003, **77**, 146.
  - [7] L. Yang, L. JiaHao and L. BaiXin, *Phys. Chem. Chem. Phys.*, 2015, **17**, 27127-27135.
  - [8] H. W. Choi, Y. H. Kim, Y. H. Rimc and Y. S. Yang, *Phys. Chem. Chem. Phys.*, 2013, **15**, 9940-9946.
  - [9] E. Amstad, F. Spaepena, D. A. Weitz, *Phys. Chem. Chem. Phys.*, 2015, **17**, 30158-30161.
  - [10] N. Bosq, N. Guigo, J. Persello, N. Sbirrazzuoli, *Phys. Chem. Chem. Phys.*, 2014, **16**, 7830-7840.
  - [11] S. Liang, D. Rozmanov, P. G. Kusalik, *Phys. Chem. Chem. Phys.*, 2011, **13**, 19856-19864.
  - [12] E. B. Moore, V. Molinero, *Phys. Chem. Chem. Phys.*, 2011, **13**, 20008-20016.
  - [13] P. Rein, ten Wolde, D. Frenkel, *Phys. Chem. Chem. Phys.*, 1999, **1**, 2191-2196.
  - [14] C. Tang, P. Harrowell, *Nature Materials*, 2013, **12**, 507-511.
  - [15] L. Zhong, J. Wang, H. Sheng, Z. Zhang, S. X. Mao, *Nature*, 2014, **512**, 177-180.
  - [16] J. A. D. Wattis and P. V. Coveney, *Phys. Chem. Chem. Phys.*, 1999, **1**, 2163-2176.
  - [17] M. C. Wilding, M. Wilson, P. F. McMillan, T. Deschampsd and B. Champagnon, *Phys. Chem. Chem. Phys.*, 2014, **16**, 22083-22096.
  - [18] C. A. Lemarchand, *J. Chem. Phys.*, 2012, **136**, 234505 1-8.
  - [19] C. A. Lemarchand, *J. Chem. Phys.*, 2013, **138**, 034506 1-10.
  - [20] A. V. Mokshin, B. N. Galimzyanov, *J. Chem. Phys.*, 2015, **142**, 104502 1-10.
  - [21] M. C. Weinberg, W. H. Poisl, L. Granasy, *C.R. Chimie*, 2002, **5**, 765-771.
  - [22] Ya. B. Zeldovich, *Acta Physicochim. URSS*, 1943, **18**, 1-92.
  - [23] V. A. Shneidman, M. C. Weinberg, *J. Chem. Phys.*, 1992, **97**, 3621-3628.
  - [24] S. A. Kukushkin, A. V. Osipov, *J. Exp. Theor. Phys.*, 1998, **86**, 1201-1208.
  - [25] F. Liu, F. Sommer, C. Bos, E. J. Mittemeijer, *International Mater. Rev.*, 2007, **52**, 193-212.
  - [26] S. A. Kukushkin, A. V. Osipov, *Progress in Surface Science*, 1996, **51**, 1-107.
  - [27] M. Dzugutov, *Phys. Rev. Lett.*, 1993, **70**, 2924-2927.
  - [28] J. Roth, A. R. Denton, *Phys. Rev. E*, 2000, **61**, 6845-6857.
  - [29] P. R. ten Wolde, M. J. Ruiz-Montero, D. Frenkel, *J. Chem. Phys.*, 1996, **104**, 9932-9947.
  - [30] P. J. Steinhardt, D. R. Nelson, M. Ronchetti, *Phys. Rev. B*, 1983, **28**, 784-805.
  - [31] A. V. Mokshin, B. N. Galimzyanov, *J. Chem. Phys.*, 2014, **140**, 024104 1-6.
  - [32] P. Hänggi, P. Talkner, M. Borkovec, *Rev. Mod. Phys.*, 1990, **62**, 251-340.
  - [33] A. V. Mokshin, B. N. Galimzyanov, *J. Phys. Chem. B*, 2012, **116**, 11959-11967.
  - [34] A. V. Mokshin, B. N. Galimzyanov, J.-L. Barrat, *Phys. Rev. E*, 2013, **87**, 062307 1-5.
  - [35] A. V. Mokshin, J.-L. Barrat, *Phys. Rev. E*, 2008, **77**,



- 021505 1-7.
- [36] A. V. Mokshin, J.-L. Barrat, *J. Chem. Phys.*, 2009, **130**, 034502 1-6.
  - [37] A. V. Mokshin, J.-L. Barrat, *Phys. Rev. E*, 2010, **82**, 021505 1-9.
  - [38] C. Valeriani, E. Sanz, D. Frenkel, *J. Chem. Phys.*, 2005, **122**, 194501 1-6.
  - [39] M. Mosayebi, E. D. Gado, P. Ilg, H. C. Öttinger, *J. Chem. Phys.*, 2012, **137**, 024504 1-11.
  - [40] C. A. Angell, *Science*, 1995, **267**, 1924-1935.
  - [41] J. Q. Broughton, G. H. Gilmer, K. A. Jackson, *Phys. Rev. Lett.*, 1982, **49**, 1496-1500.
  - [42] M. L. F. Nascimento, E. D. Zanotto, *J. Chem. Phys.*, 2010, **133**, 174701 1-10.
  - [43] T. Ogura, R. Hayami, M. Kadota, *J. Ceram. Assoc. Jpn.*, 1968, **76**, 277-284.
  - [44] S. Reinsch, M. L. F. Nascimento, R. Muller, E. D. Zanotto, *J. Non-Cryst. Solids*, 2008, **354**, 5386-5394.
  - [45] R. M. Khusnutdinoff, A. V. Mokshin, *Physica A*, 2012, **391**, 2842-2847.
  - [46] R. M. Khusnutdinoff, A. V. Mokshin, *J. Non-Cryst. Solids*, 2011, **357**, 1677-1684.
  - [47] L. Gránásy, P. F. James, *J. Chem. Phys.*, 2000, **113**, 9810-9821.
  - [48] K. F. Kelton, *Solid State Physics*, 1991, **45**, 75-177.
  - [49] M. Perez, M. Dumont, D. Acevedo-Reyes, *Acta Materialia*, 2008, **56**, 2119-2132.
  - [50] A. V. Mokshin, B. N. Galimzyanov, *J. Phys.: Conf. Series*, 2012, **394**, 012023 1-4.
  - [51] J. S. Langer, *Rev. Mod. Phys.*, 1980, **52**, 1-28.
  - [52] H. A. Wilson, *Phil. Mag.*, 1900, **50**, 238-250.
  - [53] J. Frenkel, *Phys. Z. Sowjetunion*, 1932, **1**, 498-500.
  - [54] B. N. Hale, *Phys. Rev. A*, 1986, **33**, 4156-4163.
  - [55] B. N. Hale, M. Thomason, *Phys. Rev. Lett.*, 2010, **105**, 046101 1-4.
  - [56] J. Frenkel, *Kinetic Theory of Liquids*, Oxford University Press, London, 1946.
  - [57] C. A. Angell, C. A. Scamehorn, D. J. List, J. Kieffer, *Proceedings of XV International Congress on Glass*, Leningrad, 1989.
  - [58] M. E. Blodgett, T. Egami, Z. Nussinov, K. F. Kelton, *Scientific Reports*, 2015, **5**, 13837 1-8.
  - [59] A. Kerrache, J. Horbach, K. Binder, *EPL*, 2008, **81**, 58001 1-6.
  - [60] D. Turnbull, J. C. Fisher, *J. Chem. Phys.*, 1949, **17**, 71-73.
  - [61] A. L. Greer, P. Y. Evans, R. G. Hamerton, D. K. Shanaguan, K. F. Kelton, *J. Cryst. Growth*, 1990, **99**, 38-45.
  - [62] K. F. Kelton, A. L. Greer, *J. Non-Cryst. Solids*, 1986, **79**, 295-309.
  - [63] V. Volterra, A. R. Cooper, *J. Non-Cryst. Solids*, 1985, **74**, 85-95.
  - [64] J. S. Langer, A. J. Schwartz, *Phys. Rev. A*, 1980, **21**, 948-958.
  - [65] G. T. Rengarajan, D. Enke, M. Steinharta and M. Beiner, *Phys. Chem. Chem. Phys.*, 2011, **13**, 21367-21374.